

# Fermi arcs and pseudogap emerging from dimensional crossover at the Fermi surface in $\text{La}_{2-x}\text{Sr}_x\text{CuO}_4$

P. LAZIĆ<sup>1</sup> and D. K. SUNKO<sup>2</sup>

<sup>1</sup> *R. Bošković Institute, - Bijenička cesta 54, HR-10000 Zagreb, Croatia.*

<sup>2</sup> *Department of Physics, Faculty of Science, University of Zagreb, - Bijenička cesta 32, HR-10000 Zagreb, Croatia.*

PACS 74.72.Kf – Pseudogap regime

PACS 74.72.Gh – Hole-doped cuprate superconductors

PACS 74.20.Pq – Electronic structure calculations

PACS 74.25.Jb – Electronic structure

**Abstract** – The doping mechanism and realistic Fermi surface (FS) evolution of  $\text{La}_{2-x}\text{Sr}_x\text{CuO}_4$  (LSCO) are modelled within an extensive ab-initio framework including advanced band-unfolding techniques. We show that ordinary Kohn-Sham DFT+U can reproduce the observed metal-insulator transition, when not restricted to the paramagnetic solution space. Arcs are self-doped by orbital charge transfer within the Cu–O planes, while the introduced Sr charge is strongly localized. Arc protection and the inadequacy of the rigid-band picture are consequences of a rapid change in orbital symmetry at the Fermi energy: the material undergoes a dimensional crossover along the Fermi surface, between the nodal (2D) and antinodal (3D) regions. In LSCO, this crossover accounts for FS arcs, the antinodal pseudogap, and insulating behavior in *c*-axis conductivity, all ubiquitous phenomena in high- $T_c$  cuprates. Ligand Coulomb integrals involving out-of-plane sites are principally responsible for the most striking effects observed by ARPES in LSCO.

Perovskite cuprate oxides have so far defied all efforts to understand their superconductivity (SC). They are ionic crystals, typically antiferromagnetic (AF) in the parent composition, which readily metallize upon doping. The metallization is signalled in ARPES by the Fermi arcs [1], one of the most scrutinized features of underdoped cuprates. On the other hand, the question how the out-of-plane dopands introduce charge into the planes [2] has been mostly sidelined, although the relationship between charge and dopand concentration is not simple in general [3]. The critical issue is whether the arcs appear because the doped charge is subject to 2D correlations, or the doping mechanism imposes externally that the delocalized charge first appear on the arcs.

The role of AF correlations in cuprate SC has similarly not been settled. In the superexchange mechanism [4], AF is suppressed when the bridging oxygen  $2p^6$  orbital is opened with doping. In a striking series of experiments in electron-doped cuprates [5,6], the  $2p^6$  orbital was opened instead by direct lowering of the Cu–O crystal field splitting  $\Delta_{pd}$  through removal of the apical oxygen (T/T' effect). The ensuing increase of the Cu–O covalency re-

placed the whole AF region of the phase diagram by SC. At the same time, the LTT transition in  $\text{La}_2\text{CuO}_4$  with Ba doping [7] is evidence that SC is strongly suppressed by the in-plane  $\text{O}_x\text{--O}_y$  level splitting  $\Delta_{pp}$  [8]. Both phenomena point to the interplay of covalent and ionic (crystal-field) effects involving the in-plane oxygens in the emerging metallicity and SC in cuprates.

Fermi surfaces in the cuprates cannot be modelled [9] without taking the in-plane oxygens into account either explicitly, in the Emery three-band model [10], or implicitly [11], via a next-nearest-neighbor ( $t'$ ) extension to the  $t$ – $J$  model [12]. The effective  $\text{O}_x\text{--O}_y$  hopping  $t_{pp}$  has to be rather large, even in the electron-doped cuprates [13], indicating significant particle-hole (ph) symmetry breaking in the real materials, due to the Cu–Cu-bridging O  $2p_{x,y}$  orbital being much closer in energy to the Cu  $3d^9$  than to the  $3d^8$  configuration, which is offset by the large energy  $U_d$  associated with triply-ionized  $\text{Cu}^{3+}$ .

The observed importance of ph-symmetry breaking is significant, because the O  $2p_{x,y}$  orbitals are not correlated to first order, pushing the material away from the strong-coupling (ph-symmetric, “one-band Hubbard”)

limit. However, a rigid-band tight-binding (TB) picture cannot fit FS evolution with doping [14], drawing attention to strong Coulomb interactions at low energy scales.

This crossover between ionic and metallic limits is the main interest of the present work. Focusing on LSCO, we give a unified description of the doping mechanism, arc growth, and failure of rigid bands within a single DFT+U framework. The 2D arcs appear as a 3D ionic background effect, without invoking the many-body effects in the 2D metal, which may still be responsible for the charge and spin order observed below the pseudogap temperature.

Calculations were done in Kohn-Sham DFT [15,16] with projector-augmented wave (PAW) pseudopotentials [17, 18], using the VASP software package [19,20]. The functional used was PBE [21] with +U correction [22–25]. In all calculations the cutoff of 520 eV for plane wave expansion was used together with a well converged mesh of  $8^3$   $k$ -points [26] for the smallest unit cell. The bandstructure was calculated along the high symmetry directions for the  $1\times 1\times 1$  unit cell and for larger cells an advanced zone-unfolding algorithm [27] was used as implemented in Ref. [28]. The size of the supercell limits the dopings we can achieve. Here we focus on configurations  $2\times 2\times 4$  and  $2^3$ , with doping levels 6.25% and 12.5%, respectively.

Our first result appears already in a very simple calculation, in which doping is simulated by the lack of an electron in a smeared positive background. The doping evolution is shown in Fig. 1a. The antinodal region clearly shifts in energy more quickly than the nodal one, which means that the FS evolution cannot be modeled by a rigid-band fit. However, the calculation gives a paramagnetic metal (PM) at half-filling, contrary to experiment.

It has long been understood that the LDA approach cannot give an AF insulating ground state at half-filling in the cuprates [22]. An insulating state in LSCO was obtained in the LDA+U approach [29] without gradient terms, but not a metal-insulator transition [30]. Here we revisit the issue within a generalized-gradient approximation (GGA+U) DFT approach, separating the physical aspects from the technical. LDA+U gave a band-gap which was too large, 2.3 eV [29] compared to the experimental 1.8 eV [31]. This fits with its general tendency to overbind, due to neglect of gradient terms in the electron density, so that sharply delimited charge distributions, good for binding, are unphysically “cheap” in kinetic energy. The GGA corrects this tendency by including the gradient terms.

The paramagnetic metal at half-filling in GGA+U (Fig. 1a) is by contrast a technical issue. Starting from scratch, a VASP calculation with AF-initialized magnetic moments on copper atoms leads to a PM solution. We avoid that solution by taking the converged PM solution as the initial one, and restarting the calculation with initialized AF spin configuration on the coppers. At half filling, our AF solution has a direct gap of 1.8 eV (Fig. 1c), close to the experimental one, and significant energy gain relative to the PM solution, which turns out to be less favorable thermodynamically at all dopings. Even at  $U_d = 0$

a semimetallic solution with zero density of states and a vanishing gap at  $E_f$  is thermodynamically preferred to the PM one. Our results do not depend qualitatively on the value of  $U$  at all, however when we choose the value  $U_d = 4$  eV, which fits the enthalpy of formation [32], the measured value of the band gap is obtained as a prediction. An insulating AF ground state can be modelled [33] by DFT+U in charge-transfer insulators ( $\Delta_{pd} \ll U_d \rightarrow \infty$  [4]), even if Mott insulators ( $\Delta_{pd} = U_d - \Delta_{pd} \rightarrow \infty$  [12]) cannot be. Physically, the bridging oxygens qualitatively prevent the correlation of neighboring sites, which is unavoidable in one-band models of the Mott transition, as manifested e.g. by the three-body hopping term in the  $t$ - $J$  model [12]. The oxygens open a significant alternative channel for hopping even near half-filling [34].

Standard DFT+U is highly prone to gapping instabilities if allowed to break local symmetries. When the relatively small supercell is allowed to relax fully in both spins and atomic positions, translational repetition promotes physical short-range order into unphysical long-range order, so a problem of too little metallicity appears, rather than too much. Even slight technical modifications of the DFT approach can promote gapping. Results closely conforming to experiment are obtained in the present case if one breaks the magnetic symmetry but does not allow atomic relaxation. (This means our supercell is small, not that there is no atomic relaxation in the real system.)

Introducing physical dopands now, we confirm strong localization [35] of the Sr charge. Although only 5–10% of the introduced hole charge reaches them, the planes screen the dopands metallicity: there is practically no induced charge beyond the two  $\text{CuO}_2$  planes nearest to the Sr dopand. The local effect of the Sr atom is to surround itself with negative charge, as if completing the *orbital* rather than the *charge* configuration of La. It gets screened in turn by a second layer of positive charge, so the material response to Sr is a polarization (dielectric) effect carrying a net positive charge within  $\sim 1.5$  Å of each dopand. We prove Sr charge localization in real space in Fig. 1b, showing that the dopand DOS is narrowly concentrated in a wide band gap far from  $E_f$  [36]. Furthermore, we performed a calculation at 1/8 doping with twice-as-large unit cell and two physical Sr dopands, which we placed in various positions. In all cases the distribution of charge around each dopand was identical, indicating an extremely short disorder correlation length.

There is no real-space Sr disorder in our supercell calculation. Disorder effects on the metallic arc states are expected to be minor, because of the short correlation length, Sr DOS isolation, and the orthogonality of the zone diagonal to out-of-space orbitals (see below).

A  $2,500^2$  unit-cell calculation in real space found a large amount of disorder with percolating channels [37]. Our physically similar momentum-space calculation shows what ARPES can see of that real-space picture. It seems to be a feature of out-of-plane Sr doping that metallicity initially promotes disorder, or, conversely, that AF is more

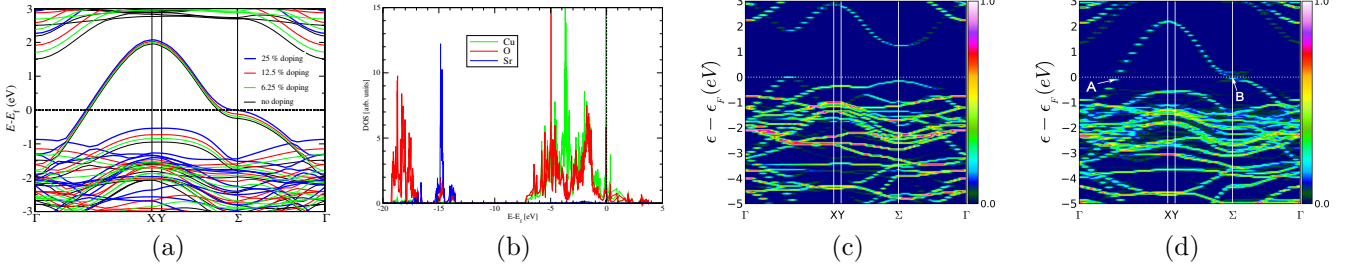


Fig. 1: (a) Gating simulation with paramagnetic starting point for four characteristic fillings, thin to thick lines: 0%, 6.25%, 12.5% and 25% doping, respectively. The shift in energy of the vH point ( $\Sigma$ ) is selectively enhanced. (b) Density of states (DOS) of the Sr dopand at 12.5% doping is concentrated around  $E - E_f = -15$  eV. (c-d) Calculations for AF starting point. Bands for  $U_d = 4$  eV at (c) zero doping and (d) 12.5% doping. The labels A and B in (d) are referred to in Fig. 3.

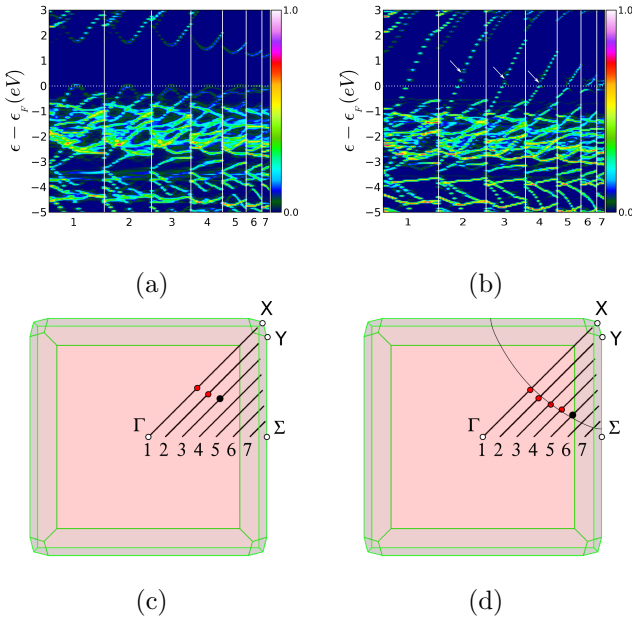


Fig. 2: Arc evolution. (a, b) Dispersions along BZ cuts from the nodal towards the antinodal point (left to right), for (a) 6.25% and (b) 12.5% doping. White arrows in (b) point to (pseudo)gap developing above the Fermi energy. (c, d) Respective cuts in the BZ. FS crossing points are marked as red dots, terminating with a black dot where the pseudogap is first observed. Thin line in (d): best fit [40] to real data [14] at 15% doping.

vulnerable to disorder than metallization [36]. Annealment by coherent hopping similarly induces disorder in a solvable model of quantum percolation in the plane [38].

Two unfolded band structures are shown in Fig. 1c and 1d, one at half-filling and the other at  $1/8$  doping. The former has a large gap and an energy gain of  $\sim 17$  meV per atom relative to the PM one. The latter has a small (pseudo)gap only around the vH singularity, and is only  $\sim 1.5$  meV per atom better than the PM one. This partial gapping is direct evidence of an arc-protection [39] effect. In the calculation the pseudogap is of mixed magnetic and orbital-disorder origin, as discussed below.

The arc evolution is further investigated in Fig. 2. We show cuts in the BZ progressing from the nodal to the antinodal point, for  $1/16$  and  $1/8$  doping. The arc extends towards the end of the zone with increasing doping, as expected from experiment [1]. Significantly, it ends with a gap opening rather abruptly: one can clearly see that the (pseudo)gap is pre-formed above the Fermi energy, so that it is already open at the point where it begins to straddle the FS. This is closely parallel to the real situation in underdoped systems, where a step-like gap is found along the FS [41, 42], as opposed to a “d-wave” gap near optimal doping. It has also been observed in BSCCO that the step-like gap is an out-of-plane effect [43]. Thus the standard DFT+U method can cross the metal-insulator (MI) transition in a manner closely resembling experiment, including the formation and growth of metallic nodal arcs, when it is not restricted to the PM solution space *a priori*.

Despite the Sr charge localization, the FS crossings in Fig. 2 conform closely but not perfectly with a Luttinger sum rule for a large FS [14], supporting the idea [2] that the majority of the charge in the plane is delocalized *in situ*, by the orbital transition  $\text{Cu}^{2+} + \text{O}^{2-} \rightleftharpoons \text{Cu}^{+} + \text{O}^{-}$ . The change in local Coulomb field when  $\text{La}^{3+}$  is replaced by  $\text{Sr}^{2+}$  expels a Cu hole onto the oxygens, closing the Cu  $3d^9$  orbital to  $3d^{10}$  and opening the O  $2p^6$  orbital to  $2p^5$  [2]. Such an *ionic doping* mechanism has recently been directly confirmed [44], while the known alternatives have been disproved: metallic alloying is excluded by the localization of the dopand charge [35], also confirmed here, while semiconductor-like impurity bands are excluded experimentally [45]. We see its effect directly by comparing charge transfers upon doping in the PM and AF solutions in Fig. 3a and 3b. In the former case, both the planar Cu and O gain holes, like in the non-interacting TB models, while in the latter, Cu *loses* holes to the bridging oxygen, as expected in the ionic doping mechanism.

The principal explanation for the above observations is given in Fig. 3c. It shows the wave-function content of the antinodal point in the zone, marked B in Fig. 1d. One can observe at least four different Cu orbital configurations (black arrows), while the wave function at the nodal FS crossing (A in Fig. 1d) consists exclusively of the planar

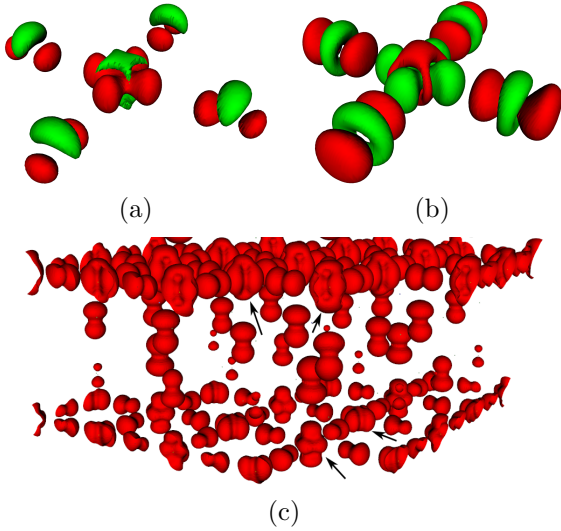


Fig. 3: (a–b) Charge-difference isosurfaces relative to zero doping. Red (green) surfaces are loci of constant  $+1(-1)\% e\text{\AA}^{-3}$ . (a)  $\text{CuO}_4$  plaquette upon  $1/8$  Sr doping, calculated with PM starting point. It predicts *both* the Cu and O planar charge differences to be positive, relative to the undoped case. (b) Charge-difference isosurfaces with AF starting point. The planar charge difference upon  $1/8$  Sr doping is negative on Cu, positive on O. (c) Isosurfaces of wave-functions at the vH point (labelled B in Fig. 1d), at  $1/8$  doping, projected onto real space. The 3D character is clearly visible. At least four different Cu orbital configurations appear (black arrows), depending on the vicinity to the Sr site. The corresponding wave-function at the nodal point (A in Fig. 1d) is strictly planar (not shown).

O  $2p_{x,y}$  and Cu  $3d_{x^2-y^2}$  orbitals (not shown). The antinodal pseudogap is characterized by strong orbital disorder, connecting to the out-of-plane atoms via the Cu  $4s$  and  $3d_{x^2-y^2}$  orbitals. This result is experimentally corroborated [43] by manipulating the arc length with out-of-plane disorder at *fixed* level of in-plane doping. The 2D metallic arcs are thus delimited by a 3D ionic background effect, obtained here in a Fermi-liquid (FL) setting by construction. The coupling to the 3D background explains why antinodal points move more quickly in energy with doping, accounting for the failure of the rigid-band approach.

It was noted previously in stoichiometric LDA calculations that the PM wave-function is 2D on the zone diagonal and 3D at the antinodal point [46], which was connected to the anisotropy in  $c$ -axis transport [47]. Here we confirm that result in a more realistic pseudogapped setting with FS arcs at finite doping. This robustness of the dimensional crossover protecting the arc is due to an orbital symmetry effect, which can be understood analytically. Out-of-plane orbitals can be subsumed in an effective  $4s$  Cu orbital, which with the usual three planar orbitals [10] makes the ensuing four-band model the minimal one with chemically realistic values of TB parameters [11]. The secular polynomial of this model factorizes along the zone diagonal ( $k_x = k_y$ ) in such a way that the dispersion

along the conducting band diagonal is uncoupled from the Cu  $4s$  orbital which is the physical conduit of out-of-plane effects into the plane. This symmetry decoupling of the diagonal is exact, unlike the *parametric* decoupling [11] of the planar dispersion for small  $t_{ps}/(\epsilon_d - \epsilon_s)$ . It is the physical mechanism of arc protection.

Interestingly, the  $\text{O}_x\text{--O}_y$  splitting  $\Delta_{pp}$  appearing in the LTT tilt [8] breaks this symmetry. It couples the states on the diagonal to out-of-plane orbitals via the Cu  $4s$  state by a mixed covalent-ionic term  $(\Delta_{pp}/2)^2 (\epsilon_d - \epsilon_k)(\epsilon_k - \epsilon_s)$  in the secular polynomial of the four-band model. The Fermi-energy ( $\epsilon_k = \epsilon_F$ ) distance from the Cu  $3d_{x^2-y^2}$  orbital  $\epsilon_d$  measures the Cu–O covalency in the conduction band, while relative to the Cu  $4s$  orbital  $\epsilon_s$  it measures the crystal-field splitting between the (hole) valence and conduction bands. The observed strong suppression of SC [7] is thus related to the removal of arc protection, lending support to the idea that SC in the underdoped cuprates first develops on the arcs [48]. One can interpret the  $T/T'$  effect [5, 6] similarly: physical removal of the apical oxygens is analogous to their removal by symmetry from the arc, cf. Fig. 3, pushing the particular material in both cases towards the 2D covalent limit [49]. Why this limit is so important for high- $T_c$  SC remains an open question.

The observation of arc protection for interstitial-oxygen doping [41, 42, 50] invites the conjecture that interstitial sites are also hidden from the zone diagonal, which is plausible if the (effective) Cu  $4s$  orbital is again the principal connection of the plane with the third dimension. We propose that a dimensional crossover along the FS is a universal property of all materials in which a FS arc is observed. Currently it seems to be a unique feature of the underdoped high- $T_c$  cuprates. (A recent report of arcs in an iridate [51] may have an alternative interpretation [52].)

Now we turn to the destruction of AF by doping. At every  $k$ -point in an AF-gapped band, there is a superposition of two states of the ungapped band,  $\phi(k)$  and  $\phi(k + Q_{AF})$ . This superposition is manifested in the real-space basis as strict staggering of magnetic moments for all the wave functions in the zone, in particular for those on the zone-diagonal Fermi surface (pocket) away from half filling. By contrast, we find real-space staggering only in the antinodal wave-functions. At  $1/8$  doping, the Cu  $3d_{x^2-y^2}$  antinodal staggered moment drops, from 0.55 magnetons at half-filling, to 0.07 in the plane nearer the Sr dopant, and to 0.17 in the farther one, with some disorder in the values. (Similar reduced values of spins were obtained in an earlier DFT calculation [53] with a different approach to spurious metallicity.) For the arc states, staggering relaxes into a longer wave, which is our model's manifestation of the nearly-AF metal observed e.g. in  $^{67}\text{Cu}$  NMR [54]. Thus the arc in the present work is not AF. As the small supercell favors AF, we cannot trust the results quantitatively, however a more realistic calculation including Sr disorder should further decrease the AF response.

The out-of-plane (3D) Coulomb effects which we study in LSCO have been experimentally [43] directly related to

the arc length in BSCCO. They appear at the antinodal region, concomitantly with remanent real-space AF staggering in the small supercell. True Sr disorder, which we cannot treat due to numerical limitations, should reduce the AF correlation length and increase the orbital disorder at the antinodal point. The connection between AF and dopand disorder is generally material-dependent [55], with the present model at one end of a continuum. The robust feature of the pseudogap here is orbital disorder, whose large (ionic) energy scales make the step-like pseudogap survive experimentally in the *high-temperature* limit [56], when smaller scales, like SC, have disappeared. At intermediate temperatures still above  $T_c$  we expect 2D metallic AF correlations to influence the pseudogap [40].

Importantly, Fermi arcs appear naturally in our calculation as an effect of lattice-symmetry breaking. The periodically repeated large supercell maps onto a small Brillouin zone, with a correspondingly complex Fermi surface due to parent-compound bands folded over many times. In this small zone all Fermi surfaces reach the zone edge by construction, because DFT+U is a one-body model. Symmetry breaking occurs by band-unfolding, which projects the small zone onto the reference parent-compound large zone, which cannot account for the dopand positions. The net effect is that the states at the Fermi energy in the small zone are “left hanging” in the large zone, i.e. one observes them as a Fermi arc. The robustness of this symmetry-breaking mechanism is attested by the fact that it already appears in our calculation with periodic dopands. Further disorder in the dopand positions can only enhance the effect. It explains the observation [43] that different arc lengths can correspond to the same concentration of mobile charge, because the length of the arc in the large zone is not simply related to the Luttinger volume enclosed by the multiple Fermi surfaces in the small zone. It also explains why Fermi arcs are observed in the highly ordered mercury cuprates, where local lattice effects of the interstitially doped oxygens in the mercury plane on the far-away copper-oxide plane are expected to be slight. The symmetry-breaking effect we describe could create an arc even if the interstitial oxygens formed a perfect superlattice, as the Sr impurities do in our calculation.

In a nutshell, arcs signify that the Coulomb effects of the dopands are not averaged out at the level of a single unit cell in the copper-oxide plane. As long as this is the case, dopand disorder is not expected to undo the effect of lattice-symmetry breaking. This effect presumably decreases as the dopand concentration increases toward optimal, signalled by the arcs reaching the edge of the large ( $\text{CuO}_2$ ) planar Brillouin zone. The physical basis of this mechanism is that the material response to doping remains dielectric between copper-oxide planes in the underdoped region. The metallicity of the arcs is due to their protection from the 3D Coulomb effects by orbital symmetry, which appears to be a highly specific feature of the cuprates.

To conclude, ligand Coulomb integrals involving out-of-

plane sites are principally responsible for the most striking effects observed by ARPES in LSCO. They gap the antinodal region extrinsically, without requiring strong 2D electron-electron correlations, usually invoked in Fermi-arc descriptions limited to the  $\text{CuO}_2$  plane. Standard Kohn-Sham DFT+U is a FL theory by construction, hence its ability to reproduce all the main features of the nodal arc, as observed in ARPES, is evidence that the 2D metallic arc states are a FL, protected by symmetry from the 3D ionic background. This result agrees with recent observations of FL  $T^2$  and  $\omega^2$  laws in transport and spectroscopic measurements [57,58]. It does not preclude further strong-coupling effects, either from copper on-site repulsion or such as the symmetry breaking by  $\Delta_{pp}$ , which may still hold the key to the SC mechanism. However, the observation of Fermi arcs does not by itself imply that the nodal metal is not a Fermi liquid.

\* \* \*

Conversations with S. Barišić, A. Fujimori, S. Mazumdar, G. Nikšić, D. Pavuna and E. Tutiš are gratefully acknowledged. We thank I. Žutić and the Center for Computational Research, University at Buffalo. P. L. thanks Paulo V. C. Medeiros, Sven Stafström and Jonas Björk for help with their BandUP code for unfolding the band-structure. D.K.S. thanks the organizers for an invitation and a stimulating time at the ECRYS-2011 Workshop on Electronic Crystals.

This work was supported by the Croatian Government under project No. 119-1191458-0512 and by the University of Zagreb grant No. 202301-202353.

## REFERENCES

- [1] YOSHIDA T., HASHIMOTO M., M. VISHIK I., SHEN Z.-X. and FUJIMORI A., *Journal of the Physical Society of Japan*, **81** (2012) 011006.
- [2] MAZUMDAR S., *A unified theoretical approach to superconductors with strong Coulomb correlations: the organics,  $\text{LiTi}_2\text{O}_4$ , electron- and hole-doped copper oxides and doped  $\text{BaBiO}_3$*  in proc. of *Interacting electrons in reduced dimensions*, edited by BAERISWYL D. and CAMPBELL D. K., (Plenum Press, New York) 1989 pp. 315–329.
- [3] OBERTELLI S. D., COOPER J. R. and TALLON J. L., *Phys. Rev. B*, **46** (1992) 14928.
- [4] BARRIQUAND F. and SAWATZKY G. A., *Phys. Rev. B*, **50** (1994) 16649.
- [5] TSUKADA A., KROCKENBERGER Y., NODA M., YAMAMOTO H., MANSKE D., ALFF L. and NAITO M., *Solid State Communications*, **133** (2005) 427.
- [6] ADACHI T., MORI Y., TAKAHASHI A., KATO M., NISHIZAKI T., SASAKI T., KOBAYASHI N. and KOIKE Y., *Journal of the Physical Society of Japan*, **82** (2013) 063713.
- [7] AXE J. D., MOUDDEN A. H., HOHLWEIN D., COX D. E., MOHANTY K. M., MOODENBAUGH A. R. and XU Y., *Phys. Rev. Lett.*, **62** (1989) 2751.

- [8] BARIŠIĆ S. and ZELENKO J., *Solid State Communications*, **74** (1990) 367.
- [9] QIMIAO SI, YUYAO ZHA, LEVIN K. and LU J. P., *Phys. Rev. B*, **47** (1993) 9055.
- [10] EMERY V. J., *Phys. Rev. Lett.*, **58** (1987) 2794.
- [11] PAVARINI E., DASGUPTA I., SAHA-DASGUPTA T., JEPSEN O. and ANDERSEN O. K., *Phys. Rev. Lett.*, **87** (2001) 047003.
- [12] ZHANG F. C. and RICE T. M., *Phys. Rev. B*, **37** (1988) 3759.
- [13] SUNKO D. K. and BARIŠIĆ S., *Phys. Rev. B*, **75** (2007) 060506.
- [14] HASHIMOTO M., YOSHIDA T., YAGI H., TAKIZAWA M., FUJIMORI A., KUBOTA M., ONO K., TANAKA K., LU D. H., SHEN Z.-X., ONO S. and ANDO Y., *Phys. Rev. B*, **77** (2008) 094516.
- [15] HOHENBERG P. and KOHN W., *Phys. Rev.*, **136** (1964) B864.
- [16] KOHN W. and SHAM L. J., *Phys. Rev.*, **140** (1965) A1133.
- [17] BLÖCHL P. E., *Phys. Rev. B*, **50** (1994) 17953.
- [18] KRESSE G. and JOUBERT D., *Phys. Rev. B*, **59** (1999) 1758.
- [19] KRESSE G. and HAFNER J., *Phys. Rev. B*, **47** (1993) 558.
- [20] KRESSE G. and FURTHMÜLLER J., *Phys. Rev. B*, **54** (1996) 11169.
- [21] PERDEW J. P., BURKE K. and ERNZERHOF M., *Phys. Rev. Lett.*, **77** (1996) 3865.
- [22] ANISIMOV V. I., ZAAENEN J. and ANDERSEN O. K., *Phys. Rev. B*, **44** (1991) 943.
- [23] ANISIMOV V. I., SOLOVYEV I. V., KOROTIN M. A., CZYŻYK M. T. and SAWATZKY G. A., *Phys. Rev. B*, **48** (1993) 16929.
- [24] LIECHTENSTEIN A. I., ANISIMOV V. I. and ZAAENEN J., *Phys. Rev. B*, **52** (1995) R5467.
- [25] DUDAREV S. L., BOTTON G. A., SAVRASOV S. Y., HUMPHREYS C. J. and SUTTON A. P., *Phys. Rev. B*, **57** (1998) 1505.
- [26] MONKHORST H. J. and PACK J. D., *Phys. Rev. B*, **13** (1976) 5188.
- [27] POPESCU V. and ZUNGER A., *Phys. Rev. B*, **85** (2012) 085201.
- [28] MEDEIROS P. V. C., STAFSTRÖM S. and BJÖRK J., *Phys. Rev. B*, **89** (2014) 041407.
- [29] ANISIMOV V. I., KOROTIN M. A., ZAAENEN J. and ANDERSEN O. K., *Phys. Rev. Lett.*, **68** (1992) 345.
- [30] ANISIMOV V. I., ARYASETIAWAN F. and LICHTENSTEIN A. I., *Journal of Physics: Condensed Matter*, **9** (1997) 767.
- [31] COOPER S. L., THOMAS G. A., MILLIS A. J., SULEWSKI P. E., ORENSTEIN J., RAPKINE D. H., CHEONG S.-W. and TREVOR P. L., *Phys. Rev. B*, **42** (1990) 10785.
- [32] HAUTIER G., ONG S. P., JAIN A., MOORE C. J. and CEDER G., *Phys. Rev. B*, **85** (2012) 155208.
- [33] CHEN Y., HUO M., SONG L. and SUN Z., *RSC Adv.*, **4** (2014) 42462.
- [34] EBRAHIMNEJAD H., SAWATZKY G. A. and BERCIU M., *Nat Phys*, **10** (2014) 951.
- [35] PERRY J. K., TAHIR-KHELI J. and GODDARD W. A., *Phys. Rev. B*, **65** (2002) 144501.
- [36] BERLIJN T., LIN C.-H., GARBER W. and KU W., *Phys. Rev. Lett.*, **108** (2012) 207003.
- [37] TAHIR-KHELI J. and GODDARD W. A., *The Journal of Physical Chemistry Letters*, **2** (2011) 2326.
- [38] SUNKO D. K., *Eur. Phys. J. B*, **43** (2005) 319.
- [39] FERRERO M., CORNAGLIA P. S., DE LEO L., PARCOLLET O., KOTLIAR G. and GEORGES A., *Phys. Rev. B*, **80** (2009) 064501.
- [40] NIKŠIĆ G., KUPČIĆ I., BARIŠIĆ O. S., SUNKO D. K. and BARIŠIĆ S., *Journal of Superconductivity and Novel Magnetism*, **27** (2014) 969.
- [41] LEE W. S., VISHIK I. M., TANAKA K., LU D. H., SASAGAWA T., NAGAOSA N., DEVEREAUX T. P., HUSSAIN Z. and SHEN Z.-X., *Nature*, **450** (2007) 81.
- [42] HE R.-H., TANAKA K., MO S.-K., SASAGAWA T., FUJITA M., ADACHI T., MANNELLA N., YAMADA K., KOIKE Y., HUSSAIN Z. and SHEN Z.-X., *Nat Phys*, **5** (2009) 119.
- [43] OKADA Y., TAKEUCHI T., BABA T., SHIN S. and IKUTA H., *Journal of the Physical Society of Japan*, **77** (2008) 074714.
- [44] PELC D., POŽEK M., DESPOJA V. and SUNKO D. K., *New Journal of Physics*, **17** (2015) 083033.
- [45] BOŽIN E. S. and BILLINGE S. J. L., *Phys. Rev. B*, **72** (2005) 174427.
- [46] ANDERSEN O. K., LIECHTENSTEIN A. I., JEPSEN O. and PAULSEN F., *J. Phys. Chem. Solids*, **56** (1995) 1573.
- [47] IOFFE L. B. and MILLIS A. J., *Phys. Rev. B*, **58** (1998) 11631.
- [48] TANAKA K., LEE W. S., LU D. H., FUJIMORI A., FUJII T., RISDIANA, TERASAKI I., SCALAPINO D. J., DEVEREAUX T. P., HUSSAIN Z. and SHEN Z.-X., *Science*, **314** (2006) 1910.
- [49] BARIŠIĆ O. S. and BARIŠIĆ S., *J. Supercond. Nov. Magn.*, **25** (2012) 669.
- [50] VISHIK I. M., BARIŠIĆ N., CHAN M. K., LI Y., XIA D. D., YU G., ZHAO X., LEE W. S., MEEVASANA W., DEVEREAUX T. P., GREVEN M. and SHEN Z.-X., *Phys. Rev. B*, **89** (2014) 195141.
- [51] KIM Y. K., KRUPIN O., DENLINGER J. D., BOSTWICK A., ROTENBERG E., ZHAO Q., MITCHELL J. F., ALLEN J. W. and KIM B. J., *Science*, **345** (2014) 187.
- [52] DE LA TORRE A., HUNTER E. C., SUBEDI A., MCKEOWN WALKER S., TAMAI A., KIM T. K., HOESCH M., PERRY R. S., GEORGES A. and BAUMBERGER F., *Phys. Rev. Lett.*, **113** (2014) 256402.
- [53] BARBIELLINI B. and JARLBORG T., *Phys. Rev. Lett.*, **101** (2008) 157002.
- [54] MORIYA T., TAKAHASHI Y. and UEDA K., *Journal of the Physical Society of Japan*, **59** (1990) 2905.
- [55] ANDERSEN B. M., HIRSCHFELD P. J., KAMPF A. P. and SCHMID M., *Phys. Rev. Lett.*, **99** (2007) 147002.
- [56] RAZZOLI E., DRACHUCK G., KEREN A., RADOVIC M., PLUMB N. C., CHANG J., HUANG Y.-B., DING H., MESOT J. and SHI M., *Phys. Rev. Lett.*, **110** (2013) 047004.
- [57] BARIŠIĆ N., CHAN M. K., LI Y., YU G., ZHAO X., DRESSEL M., SMONTARA A. and GREVEN M., *PNAS*, **110** (2013) 12235.
- [58] MIRZAEI S. I., STRICKER D., HANCOCK J. N., BERTHOD C., GEORGES A., VAN HEUMEN E., CHAN M. K., ZHAO X., LI Y., GREVEN M., BARIŠIĆ N. and VAN DER MAREL D., *PNAS*, **110** (2013) 5774.